Original Article

Construction and validation of deep learning model for cachexia in extensive-stage small cell lung cancer patients treated with immune checkpoint inhibitors: a multicenter study

Ruiting Song[1,2#]^, Butuo Li[1#], Xiaoqing Wang[3], Xinyu Fan[1], Zhonghang Zheng[4], Yawen Zheng[5], Junyi He[1,6], Chunni Wang[1], Linlin Wang[1]^

[1]Department of Radiation Oncology, Shandong Cancer Hospital and Institute, Affiliated to Shandong First Medical University and Shandong Academy of Medical Sciences, Jinan, China; [2]Shandong First Medical University and Shandong Academy of Medical Sciences, Jinan, China; [3]Department of Portal Hypertension, Shandong Public Health Clinical Center, Shandong University, Jinan, China; [4]Department of Nuclear Medicine, Shandong First Medical University Affiliated Jining First People's Hospital, Jining, China; [5]Department of Obstetrics and Gynecology, Qilu Hospital of Shandong University, Jinan, China; [6]Shandong University Cancer Center, Jinan, China

Contributions: (I) Conception and design: L Wang; (II) Administrative support: R Song, B Li; (III) Provision of study materials or patients: X Wang, X Fan, Z Zheng, Y Zheng, J He, C Wang, L Wang; (IV) Collection and assembly of data: R Song, X Fan, Z Zheng; (V) Data analysis and interpretation: R Song, B Li; (VI) Manuscript writing: All authors; (VII) Final approval of manuscript: All authors.

[#]These authors contributed equally to this work.

Correspondence to: Dr. Linlin Wang, PhD. Department of Radiation Oncology, Shandong Cancer Hospital and Institute, Affiliated to Shandong First Medical University and Shandong Academy of Medical Sciences, Jiyan Road 440, Jinan 250117, China. Email: wanglinlinatjn@163.com.

Background: Cachexia is observed in around 60% of patients with extensive-stage small cell lung cancer (ES-SCLC) and may play an important role in the development of resistance to immunotherapy. This study aims to evaluate the influence of cachexia on the effectiveness of immunotherapy, develop and assess a deep learning (DL)-based prediction model for cachexia, as well as its prognostic value.

Methods: The analysis encompassed ES-SCLC patients who received the combination of first-line immunotherapy and chemotherapy from Shandong Cancer Hospital and Institute, Qilu Hospital, and Jining First People's Hospital. Survival analysis was conducted to examine the correlation between cachexia and the efficacy of immunotherapy. Medical records and computed tomography (CT) images of the third lumbar vertebra (L3) level were collected to construct the clinical model, radiomics, and DL models. The receiver operating characteristic (ROC) curve analysis was conducted to assess and analyze the efficacy of various models in detecting and evaluating the risk of cachexia.

Results: A total of 231 ES-SCLC patients were enrolled in the study. Cachexia was related to inferior progression-free survival (PFS) and overall survival (OS). In internal and external validation cohorts, the area under the curve (AUC) of the DL model were 0.73 and 0.71. Conversely, the radiomics model in external validation cohort recorded an AUC of 0.67, highlighting the superior performance of the DL model and its demonstrated capability for effective generalization in external validation. All patients were categorized into two groups, namely high risk and low risk using the DL model. It was shown that patients with low-risk cachexia were associated with significantly prolonged PFS and OS.

Conclusions: The DL model not only had better performance in predicting cachexia but also correlated with survival outcomes of ES-SCLC patients who receiving initial immunotherapy.

Keywords: Cachexia; small cell lung cancer (SCLC); immunotherapy; radiomics; deep learning (DL)

^ ORCID: Ruiting Song, 0009-0009-3124-6648; Linlin Wang, 0000-0002-2231-6642.

Submitted Jun 24, 2024. Accepted for publication Oct 12, 2024. Published online Nov 28, 2024.
doi: 10.21037/tlcr-24-543
View this article at: https://dx.doi.org/10.21037/tlcr-24-543

Introduction

Small cell lung cancer (SCLC) constitutes around 15% to 17% of all lung cancer patients (1,2). At the time of diagnosis, over 60% of patients exhibit extensive-stage SCLC (ES-SCLC), with the median survival ranging from 8 to 13 months. Additionally, the five-year survival rate is less than 7% in the era of chemotherapy (3,4). Immunotherapy has represented a new landmark in the therapeutic approach of ES-SCLC. IMpower133 and CASPIAN have indicated a two-month improvement in the overall survival (OS) for patients with ES-SCLC by the administration of programmed death ligand 1 (PD-L1) checkpoint inhibitors in combination with chemotherapy alone (5-7). However, it is crucial to identify which patients will get significant and long-lasting benefits from immunotherapy, as only a minority of patients experience a complete and durable response (8).

Cachexia, a multifaceted illness characterized by gradual weight loss and muscle wasting (9), afflicts up to 80% of patients with advanced cancer (10) and contributes to over 20% of cancer-related deaths (11). Tumor-related cachexia impacts the ability of the adaptive immune system to mount antigen-specific responses, which might result in the reduction of the effectiveness of immunotherapy in cancer patients (12). It has been observed that cachexia can promote primary resistance to immunotherapy in a variety of malignancies, such as non-small cell lung cancer (NSCLC), melanoma, bladder cancer and others (13). However, the impact of cachexia on the effectiveness of immunotherapy in ES-SCLC patients remains uncertain.

Weight loss has been associated with a poor response to treatment and a shorter survival time in SCLC patients (14). The early identification of ES-SCLC patients who might suffer from cachexia could help the early initiation of intervention to retard the progress of cachexia. Several markers, including sarcopenia, cachexia score, and nutritional indicators (15,16), have been investigated to identify patients at high risk of developing cachexia. However, there is no definitive predictive index for the onset of cachexia in ES-SCLC patients.

Previous research has suggested that the intercommunication mechanism between skeletal muscle and immune cells may play a role in the pathophysiology of cachexia (17). Because of their linear association with systemic equivalents, muscles at the third lumbar vertebra (L3) slice are widely used as a reference location for measuring sarcopenia (18). Radiomics features of skeletal muscles using magnetic resonance imaging (MRI), computed tomography (CT), or positron emission tomography/CT (PET/CT) have promise in discerning the likelihood of cachexia and predicting the efficacy of immunotherapy in NSCLC patients. Deep learning (DL) can directly learn from medical images and automatically extract valuable features for model construction. The expert performance has been demonstrated in a variety of tasks, such as the differentiation of benign and malignant tumors (19), cancer grading (20), and lymph node metastasis (21) prediction. In this study, we intended to evaluate the influence of cachexia on the effectiveness of immunotherapy, and to develop a DL model to predict the incidence of cachexia during immunotherapy treatment, and assess its prognostic value. We present this article in accordance with the TRIPOD reporting checklist (available at https://tlcr.amegroups.com/article/view/10.21037/tlcr-24-543/rc).

Highlight box

Key findings

- The deep learning (DL) model accurately predicts cachexia and its association with survival in extensive-stage small cell lung cancer (ES-SCLC) patients receiving first-line immunotherapy.

What is known and what is new?

- Cachexia affects around 60% of ES-SCLC patients and may contribute to resistance to immunotherapy.
- This study first demonstrates that cachexia reduces the effectiveness of immunotherapy in ES-SCLC and introduces a highly effective DL model to predict cachexia, which strongly correlates with immunotherapy outcomes.

What is the implication, and what should change now?

- DL model can serve as a novel tool to assist clinicians in early detection of cachexia, enabling timely nutritional guidance and clinical intervention.

Methods

Study population

This research, a retrospective and multi-institutional investigation, received approval from the Ethics Committee of Shandong Cancer Hospital and Institute (No. 2023010002) and the Institutional Review Board at each participating hospital. All participating institutions were informed and agreed on the study. The research was conducted in accordance with the Declaration of Helsinki (as revised in 2013), and given that it is a retrospective study, individual consent for this retrospective analysis was waived. From January 2018 to April 2022, ES-SCLC patients receiving immunotherapy were included in the study from Shandong Cancer Hospital and Institute, Qilu Hospital, and Jining First People's Hospital. Immunotherapy primarily refers to at least four cycles of platinum-based drugs (cisplatin or carboplatin) plus etoposide in combination with durvalumab or atezolizumab, followed by maintenance therapy with durvalumab or atezolizumab monotherapy. The follow-up deadline was January 1, 2023. The minimum follow-up period was six months, while the maximum depended on the time of death. The inclusion criteria were as follows: (I) radiologically and histologically confirmed ES-SCLC; (II) receiving at least two cycles of immunotherapy; (III) with acceptable CT images before the initiation of immunotherapy; (IV) Eastern Cooperative Oncology Group (ECOG) 0–2. The following were the detailed exclusion criteria: (I) more than 3-month interval between the CT image and the initiation of immunotherapy; (II) a follow-up period of fewer than six months; (III) with another primary tumor; (IV) absence of weight data during immunotherapy. Patients from Shandong Cancer Hospital and Institute were randomly allocated into two cohorts, namely the training and internal validation cohort, using a ratio of 7:3. And patients from Qilu Hospital and Jining First People's Hospital were included in external validation cohort to validate the effectiveness of models.

The researchers obtained clinical data from the medical records, including gender, age, body mass index (BMI), smoking history, liver metastases, brain metastases, bone metastases, the number of metastases and hematological parameters results. These data were gathered prior to the initiation of immunotherapy. The cut-off of the age and hematological parameters were determined by maximizing the Youden index of the training cohort. Besides, contrast-enhanced arterial phase CT images of the chest and upper abdomen were collected within a month before the start of immunotherapy. Cachexia was characterized as a reduction in body weight over 5% within the preceding six-month period or a weight loss above 2% with a BMI less than 20 kg/m^2 (22). Tumor response was assessed in accordance with the solid tumor Response Evaluation Criteria (RECIST1.1). Progression-free survival (PFS) was defined from the initiation of immunotherapy and the earliest occurrence of disease progression, as determined by RECIST1.1, or death from any cause. If neither progression nor death occurred, the date of the last follow-up was used as the censoring point for PFS. OS was defined from the initiation of immunotherapy to the death from any cause, with patients still alive at the last follow-up being censored at that time.

Image pre-processing and feature extraction

The regions of interest (ROIs) in the CT imaging at L3 slice were identified and segmented encompassing muscles such as psoas, transversus abdominus, paraspinal muscles, external and internal obliques, and rectus abdominus (23). Semi-automated segmentation was performed to identify ROIs (24). The range of Hounsfield units for skeletal muscle was set from 29 to 150, and misclassified structures such as vertebrae, ribs, fat, and organs were manually rectified. The ROIs for radiomics analysis was defined by two radiologists over five years of clinical expertise blinded to the clinical results. The Pyradiomics Python packages were used to extract radiomics features from the ROIs. The intraclass correlation coefficient (ICC) was used to assess reproducibility between observers, was determined between the features from two radiologists, and features with ICC >0.8 were chosen to assure segmentation robustness. The radiomics features were then normalized using z-score.

Radiomics feature selection and rad score (RS) construction

A regression analysis using the least absolute shrinkage and selection operator (LASSO) was performed to identify the strongest predictive features for cachexia. Then, a five-fold cross-validation was employed to determine the optimal penalty parameter (λ) in LASSO. The radiomic characteristics that had non-zero coefficients were conducted to construct radiomic labels. Subsequently, the RS was generated by a linear combination of these features, with each component being assigned a weight based on its

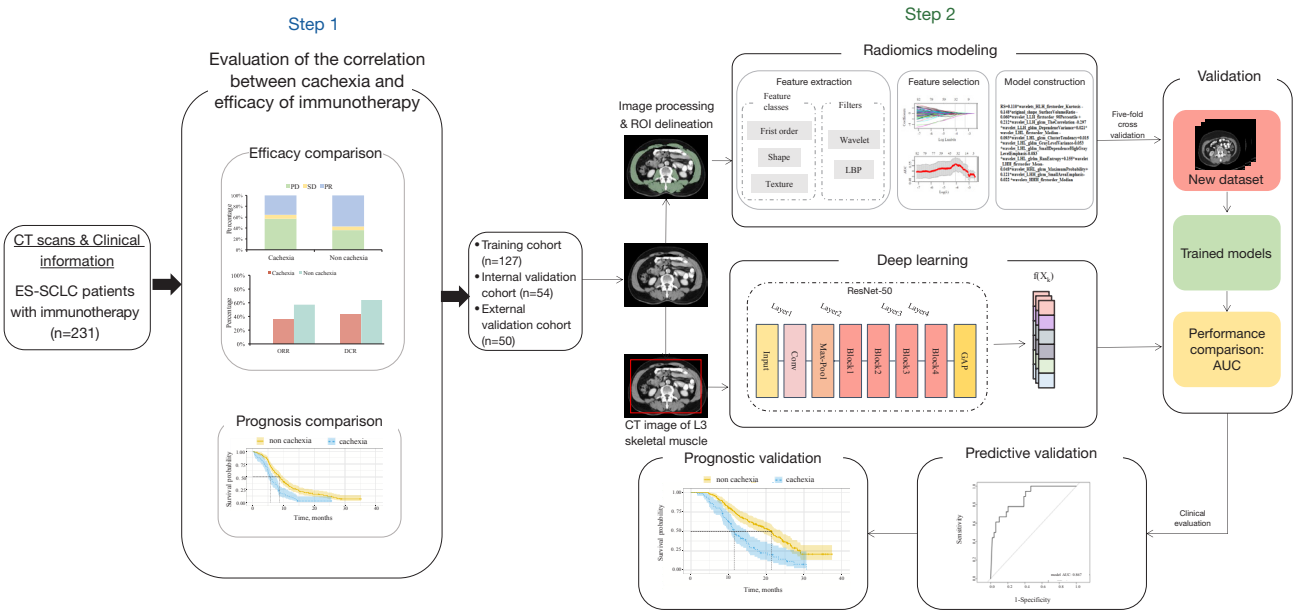

Figure 1 The overall pipeline of the study including two main steps. Firstly, the correlation between cachexia and prognosis of ES-SCLC patients receiving immunotherapy was determined. Then the clinical model, radiomics model and DL model were constructed for the prediction of cachexia. A comparison of the performance of the three models, in terms of both cachexia prediction and prognosis, was performed in validation cohort. The red box highlights the key sampling area for training the DL model, specifically focusing on the automatic feature extraction of images at the L3, including skeletal muscle and surrounding tissues and organs. This approach differs from the radiomics model, where image features are extracted solely from the skeletal muscle at the L3 level (the skeletal muscle region is emphasized in green). CT, computed tomography; ES-SCLC, extensive-stage small cell lung cancer; PD, progressive disease; SD, stable disease; PR, partial response; ORR, objective response rate; DCR, disease control rate; L3, third lumbar vertebra; ROI, region of interest; LBP, local binary patterns; Conv, convolutional layer; GAP, global average pooling; AUC, area under the curve; DL, deep learning.

corresponding coefficients.

Construction of DL model

For the binary classification task of predicting cachexia, a DL model was created using the ResNet-50, which had been pretrained in the ImageNet dataset. The input was a CT image of the L3 vertebrae resampled into a 224×224 matrix, and the outcome variable was the occurrence of cachexia. Subsequently, cross-entropy loss is utilized to measure the performance of models. The training procedure adopts an adaptive moment estimation (Adam) optimizer. For steady training, it is recommended to assign a learning rate of 0.0001 and a momentum term β to 0.5. The batch size was configured to 50, whereas the epochs were set to 500. The model parameters were updated through backpropagation.

Validation and comparison of the performance between different models

The predictive effect of clinical, radiomics, and DL models for cachexia was assessed using receiver operating characteristic (ROC) curve analysis. Furthermore, survival analysis was conducted to validate the potential correlation between risk stratification based on the predictive models for cachexia and the efficacy of immunotherapy. The complete procedure of this research is shown in *Figure 1*.

Statistical analysis

The χ^2 test was used to compare the variations of training, internal validation, and external validation. In addition, the χ^2 test was utilized to determine if patients with cachexia can respond differently to immunotherapy. To confirm

the connection between cachexia and survival in ES-SCLC patients undergoing immunotherapy, Kaplan-Meier (KM) survival analysis was performed. To investigate the independent predictors of survival in ES-SCLC patients undergoing immunotherapy, univariate and multivariate Cox analyses were performed. Univariate logistic analysis was employed to assess the association between clinical and hematological parameters and cachexia. To construct the clinical signature, parameters with P<0.05 were added in multivariate logistic analysis. All statistical analyses were two-sided, P<0.05 was used to determine statistical significance while 95% confidence interval (CI) were calculated at the same time. IBM SPSS Statistics version 23.0 was used for data processing and statistical analysis. Survival curves were performed in R version 4.1.1 using the "survminer" and "Survival" packages.

Results

Baseline characteristics of included patients

The study had a sample of 231 patients (183 males and 48 females) with an average age of 61.2±8.2 years. Among them, 181 patients from Shandong Cancer Hospital were allocated into a training cohort group (n=127) and an internal validation cohort (n=54). Meanwhile, the external validation cohort comprised 50 patients from Qilu Hospital and Jining First People's Hospital. The median PFS (mPFS) was 7.8 months (95% CI: 6.9–8.7), and the median OS (mOS) was 16.9 months (95% CI: 14.1–19.8). There were 70 patients experiencing cachexia among all 231 patients. According to *Table 1*, no statistically significant differences were found in the clinical and haematological characteristics among the three cohorts.

The association between cachexia and the efficacy of immunotherapy

As shown in *Figure 2A*,*2B*, among all 231 patients, those with cachexia were associated with significantly decreased disease control rate (DCR) (63.9% *vs.* 42.9%, P=0.003) and objective response rate (ORR) (57.1% *vs.* 35.7%, P=0.003). Survival analysis indicated inferior PFS (mPFS 5.7 *vs.* 8.8 months, P<0.001) and OS (mOS 11.5 *vs.* 21.4 months, P<0.001) for patients with cachexia (*Figure 2C*,*2D*). Multivariate

Table 1 Baseline characteristics of included patients

Clinical factors	Training cohort (n=127), n (%)	Internal validation cohort (n=54)		External validation cohort (n=50)	
		n (%)	P	n (%)	P
Gender			0.48		0.69
Male	100 (78.7)	45 (83.3)		38 (76.0)	
Female	27 (21.3)	9 (16.7)		12 (24.0)	
Age (years)			0.92		0.08
≤52	22 (17.3)	9 (16.7)		3 (6.0)	
>52	105 (82.7)	45 (83.3)		47 (94.0)	
Smoking history			0.43		0.52
Yes	72 (56.7)	34 (63.0)		31 (62.0)	
No	55 (43.3)	20 (37.0)		19 (38.0)	
Bone metastasis			0.3		0.6
Yes	46 (36.2)	24 (44.4)		16 (32.0)	
No	81 (63.8)	30 (55.6)		34 (68.0)	
Liver metastasis			0.86		0.24
Yes	50 (39.4)	22 (40.7)		15 (30.0)	
No	77 (60.6)	32 (59.3)		35 (70.0)	

Table 1 (*continued*)

Table 1 (*continued*)

Clinical factors	Training cohort (n=127), n (%)	Internal validation cohort (n=54)		External validation cohort (n=50)	
		n (%)	P	n (%)	P
Brain metastasis			0.53		0.27
Yes	57 (44.9)	27 (50.0)		27 (54.0)	
No	70 (55.1)	27 (50.0)		23 (46.0)	
Pancreatic metastasis			0.33		0.52
Yes	5 (4.0)	4 (7.4)		1 (2.0)	
No	122 (96.0)	50 (92.6)		49 (98.0)	
Adrenal metastasis			0.17		0.12
Yes	14 (11.0)	10 (18.5)		10 (20.0)	
No	113 (89.0)	44 (81.5)		40 (80.0)	
Cachexia			0.94		0.21
Yes	36 (28.3)	15 (27.8)		19 (38.0)	
No	91 (71.7)	39 (72.2)		31 (62.0)	
TP (g/L)			0.64		0.54
≤68	47 (37.0)	18 (33.3)		21 (42.0)	
>68	80 (63.0)	36 (66.7)		29 (58.0)	
PA (g/L)			0.68		0.69
≤0.187	27 (21.3)	10 (18.5)		12 (24.0)	
>0.187	100 (78.7)	44 (81.5)		38 (76.0)	
LDH (U/L)			0.24		0.43
≤273	89 (70.1)	33 (61.1)		38 (76.0)	
>273	38 (29.9)	21 (38.9)		12 (24.0)	
WBC (10^9/L)			0.18		0.18
≤4.33	24 (18.9)	15 (27.8)		14 (28.0)	
>4.33	103 (81.1)	39 (72.2)		36 (72.0)	
ALC (10^9/L)			0.08		0.71
≤1.89	93 (73.2)	46 (85.2)		38 (76.0)	
>1.89	34 (26.8)	8 (14.8)		12 (24.0)	
NE (10^9/L)			0.19		0.31
≤2.34	22 (17.3)	14 (25.9)		12 (24.0)	
>2.34	105 (82.7)	40 (74.1)		38 (76.0)	

TP, total protein; PA, prealbumin; LDH, lactate dehydrogenase; WBC, white blood cell count; ALC, absolute lymphocyte count; NE, neutrophils.

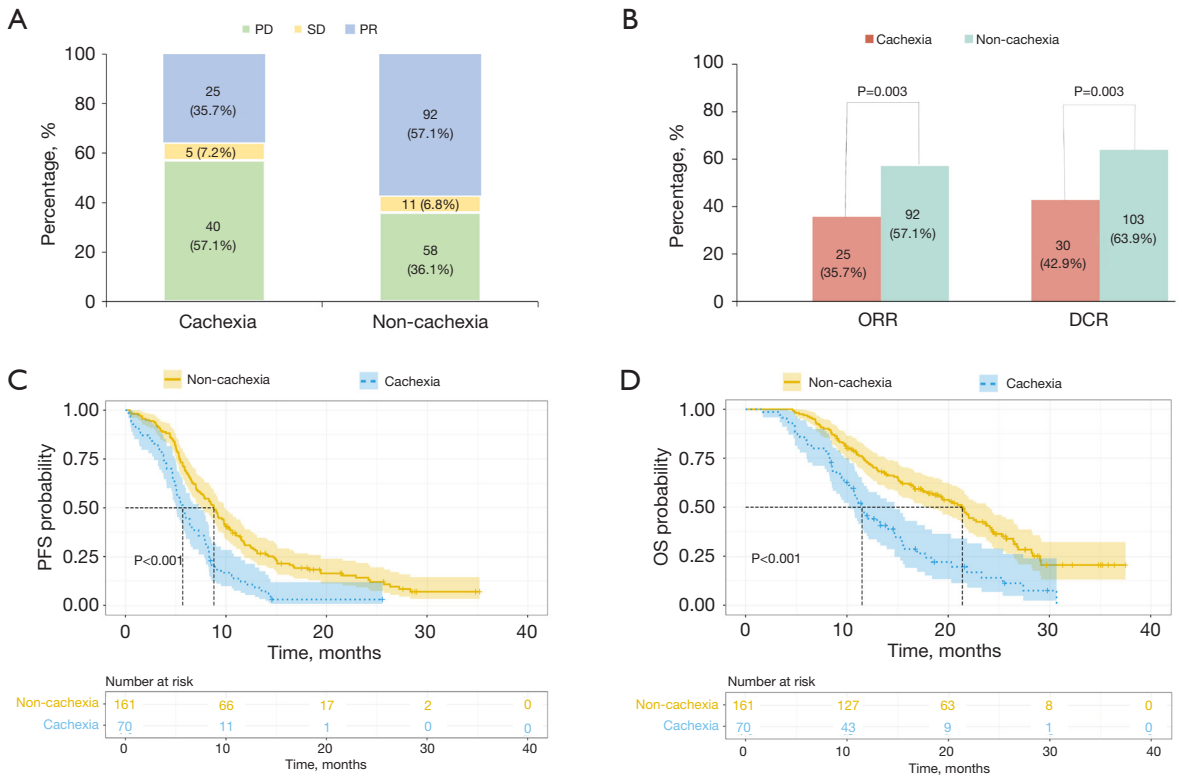

Figure 2 The association between cachexia and the efficacy of immunotherapy for ES-SCLC patients. The distribution of treatment response between cachexia and non-cachexia groups (A), differences in response rate between cachexia and non-cachexia groups (B), the Kaplan-Meier curves of PFS (C) and OS (D) between patients with or without cachexia. PD, progressive disease; SD, stable disease; PR, partial response; ORR, objective response rate; DCR, disease control rate; PFS, progression-free survival; OS, overall survival; ES-SCLC, extensive-stage small cell lung cancer.

Cox regression analysis revealed that cachexia was an independent clinical predictor for PFS (*Table 2*) and OS in ES-SCLC patients who undergo immunotherapy using multivariate Cox regression analysis (*Table 3*).

Construction of clinical prediction model

According to the univariate logistic regression analysis, lactate dehydrogenase (LDH), absolute lymphocyte count (ALC), white blood cell count (WBC), neutrophils (NE), and prealbumin (PA) levels were found to be linked with the incidence of cachexia (*Table 4*). The clinical prediction model was built using multivariate logistic regression, which revealed that ALC [odds ratio (OR) =3.43, 95% CI: 1.37–8.61, P=0.009] and PA (OR =0.27, 95% CI: 0.10–0.74, P=0.01) were independent predictors of cachexia. The area under the curve (AUC) of the clinical prediction model for cachexia in the training cohort was 0.71 (95% CI: 0.62–0.81), 0.63 (95% CI: 0.52–0.74) in the internal validation cohort, and 0.63 (95% CI: 0.46–0.79) in the external validation cohort (*Table 5*).

Development of the RS and DL model

A total of 874 radiomic features from each patient were extracted using pyradiomics. After removing features with excessive missing values and those with an ICC <0.8, a set of 666 robust features was chosen and normalized utilizing the z-score. Subsequently, these features were subjected to LASSO regression analysis, and 14 nonzero radiomic features were selected. The RS was then calculated using the following method based on the weights of these 14 features: RS = 0.110 × wavelets_HLH_firstorder_Kurtosis – 0.148 × original_shape_SurfaceVolumeRatio – 0.060 × wavelet_LLH_firstorder_90Percentile + 0.212 × wavelet_LLH_glcm_TheCorrelation – 0.297 × wavelet_LLH_gldm_

Table 2 Univariate and multivariate Cox proportional hazards regression analysis for PFS of ES-SCLC patients receiving immunotherapy

Variable	Univariable analysis			Multivariable analysis		
	HR	95% CI	P	HR	95% CI	P
Age	0.89	0.61–1.30	0.54			
Gender	1.29	0.91–1.83	0.15			
Cachexia	2.07	1.53–2.79	<0.001	2.07	1.52–2.83	<0.001
Smoking history	1.28	0.96–1.70	0.10			
Bone metastasis	2.30	1.73–3.07	<0.001	1.73	1.24–2.41	0.001
Liver metastasis	1.84	1.39–2.43	<0.001	1.54	1.12–2.11	0.007
Brain metastasis	1.35	1.02–1.79	0.03			
Pancreatic metastasis	1.71	0.90–3.25	0.10			
Adrenal metastasis	1.45	1.00–2.12	0.052			
TP	1.01	0.76–1.34	0.96			
LDH	1.81	1.35–2.43	<0.001			
ALC	0.78	0.56–1.09	0.14			
WBC	1.18	0.84–1.65	0.36			
NE	0.93	0.66–1.30	0.67			
PA	1.07	0.77–1.50	0.69			

PFS, progression-free survival; ES-SCLC, extensive-stage small cell lung cancer; HR, hazard ratio; 95% CI, 95% confidence interval; TP, total protein; LDH, lactate dehydrogenase; ALC, absolute lymphocyte count; WBC, white blood cell count; NE, neutrophils; PA, prealbumin.

Table 3 Univariate and multivariate Cox proportional hazards regression analysis of OS of ES-SCLC patients receiving immunotherapy

Variable	Univariable analysis			Multivariable analysis		
	HR	95% CI	P	HR	95% CI	P
Age	0.84	0.55–1.29	0.43			
Gender	1.49	0.98–2.28	0.06			
Cachexia	2.26	1.62–3.17	<0.001	2.76	1.94–3.93	<0.001
Smoking history	1.40	1.01–1.95	0.04			
Bone metastasis	2.05	1.48–2.83	<0.001	1.44	1.01–2.07	0.04
Liver metastasis	2.14	1.56–2.94	<0.001	2.11	1.48–3.00	<0.001
Brain metastasis	1.17	0.85–1.60	0.34			
Pancreatic metastasis	1.81	0.89–3.71	0.10			
Adrenal metastasis	1.67	1.10–2.56	0.02	1.63	1.06–2.52	0.03
TP	0.72	0.52–1.00	0.048	0.67	0.48–0.94	0.02
LDH	1.85	1.33–2.59	<0.001			
ALC	0.78	0.52–1.15	0.21			
WBC	1.50	1.00–2.27	0.051			
NE	1.25	0.83–1.89	0.28			
PA	0.77	0.53–1.12	0.17			

OS, overall survival; ES-SCLC, extensive-stage small cell lung cancer; HR, hazard ratio; 95% CI, 95% confidence interval; TP, total protein; LDH, lactate dehydrogenase; ALC, absolute lymphocyte count; WBC, white blood cell count; NE, neutrophils; PA, prealbumin.

Table 4 Univariate and multivariate logistic regression analysis for the cachexia in ES-SCLC patients receiving immunotherapy

Variable	Univariable analysis			Multivariable analysis		
	OR	95% CI	P	OR	95% CI	P
Age	0.40	0.15–1.02	0.06			
Gender	1.17	0.45–3.06	0.75			
Smoking history	1.29	0.59–2.83	0.53			
Bone metastasis	1.17	0.53–2.60	0.69			
Liver metastasis	0.83	0.37–1.83	0.64			
Brain metastasis	1.14	0.53–2.47	0.74			
Pancreatic metastasis	1.73	0.28–10.78	0.56			
Adrenal metastasis	1.01	0.30–3.46	0.98			
TP	1.78	0.77–4.13	0.18			
LDH	2.51	1.11–5.66	0.03			
ALC	3.90	1.68–9.02	0.002	3.43	1.37–8.61	0.009
WBC	11.84	1.53–91.34	0.02			
NE	10.50	1.36–81.30	0.02			
PA	0.26	0.11–0.64	0.003	0.27	0.10–0.74	0.01

ES-SCLC, extensive-stage small cell lung cancer; OR, odds ratio; 95% CI, 95% confidence interval; TP, total protein; LDH, lactate dehydrogenase; ALC, absolute lymphocyte count; WBC, white blood cell count; NE, neutrophils; PA, prealbumin.

Table 5 Comparison of predictive performance between different models

Model	Training cohort		Internal validation cohort		External validation cohort	
	AUC	95% CI	AUC	95% CI	AUC	95% CI
Clinical model	0.71	0.62–0.81	0.63	0.52–0.74	0.63	0.46–0.79
Radiomics model	0.79	0.70–0.88	0.78	0.65–0.90	0.67	0.52–0.82
DL model	–	–	0.73	0.59–0.84	0.71	0.56–0.83

AUC, area under the curve; 95% CI, 95% confidence interval; DL, deep learning.

DependenceVariance + 0.021 × wavelet_LHL_firstorder_Median – 0.093 × wavelet_LHL_glcm_ClusterTendency + 0.015 × wavelet_LHL_gldm_GrayLevelVariance – 0.053 × wavelet_LHL_gldm_SmallDependenceHighGrayLevelEmphasis – 0.083 × wavelet_LHL_glrlm_RunEntropy + 0.155 × wavelet_LHH_firstorder_Mean – 0.048 × wavelet_HHL_glcm_MaximumProbability + 0.121 × wavelet_LHH_glcm_SmallAreaEmphasis – 0.022 × wavelets_HHH_firstorder_Median. The AUC of RS for predicting the risk of cachexia was 0.79 (95% CI: 0.70–0.88) in the training cohort, 0.78 (95% CI: 0.65–0.90) in the internal validation cohort, and 0.67 (95% CI: 0.52–0.82) in the external validation cohort (*Table 5*).

The ResNet-50 model was adopted to train the DL model, and the model with the higher accuracy in the validation cohort was saved after 500 epochs. The patients were categorized into high-risk and low-risk cachexia using the DL model. In the internal and external validation cohorts, the AUC of the DL model was 0.73 (95% CI: 0.59–0.84) and 0.71 (95% CI: 0.56–0.83), respectively (*Figure 3*).

Comparison and validation of predictive models

In terms of the accuracy, the DL model outperformed the RS in the external validation cohort, demonstrating

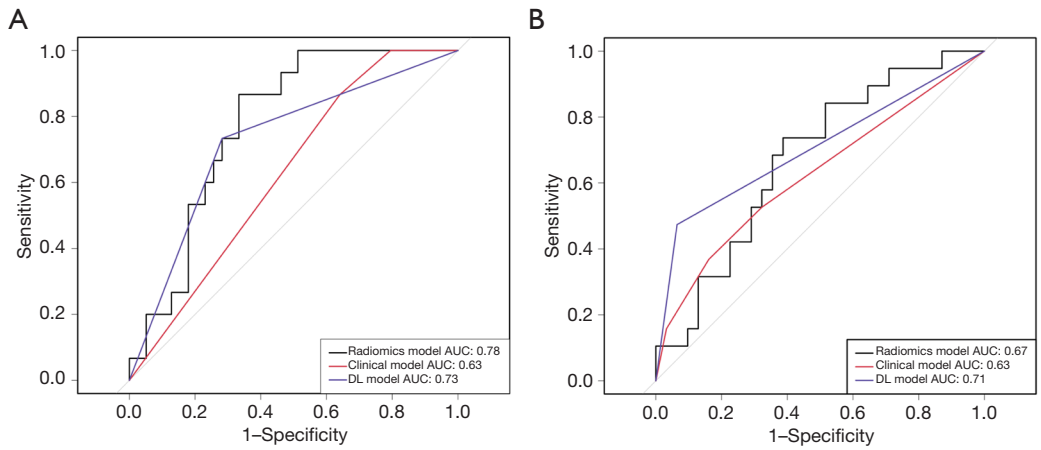

Figure 3 ROC curves between different models for predict cachexia. The comparison of ROC curves between radiomics model, DL model and clinical models in the internal (A) and external validation cohorts (B), respectively. AUC, area under the curve; DL, deep learning; ROC, receiver operating characteristic.

improved robustness and external applicability (*Table 5*). KM curve was conducted to assess the correlation between the prediction of DL model and the survival of patients. In the internal validation cohort, patients in the high-risk group were linked with inferior PFS than the low-risk group (mPFS 5.1 *vs.* 8.7 months, P=0.006) (*Figure 4A*) and OS (mOS 14.7 *vs.* 23.3 months, P=0.046) (*Figure 4B*). VA similar result was also shown in external validation cohort, with the significantly inferior PFS (mPFS 4.7 *vs.* 11.5 months, P=0.02) (*Figure 4C*) and OS (mOS 10.3 *vs.* 15.5 months, P=0.045) (*Figure 4D*) in the high-risk group.

Discussion

To the utmost of our understanding, this study represents the inaugural attempt to investigate the correlation between cachexia and the efficacy of immunotherapy in ES-SCLC patients. The result indicated that the correlation does exist between cachexia and poor survival of patients. Early detection of cachexia is critical for immunotherapy precision treatment. Therefore, we created predictive models for cachexia based on clinical and radiomics features. The findings suggested that DL model performed better, which was also related to the efficacy of immunotherapy.

In this study, 28.1% of ES-SCLC patients experienced cachexia before receiving first-line immune checkpoint inhibitors (ICIs) and chemotherapy. This study firstly found that cachexia was associated with poor PFS and OS of immunotherapy in ES-SCLC patients. Previous studies also highlighted the association between cachexia and inferior efficacy of immunotherapy in various cancers (25-27). In patients with NSCLC treated with ICIs, those who develop cachexia have lower survival rates (28-30), especially among patients with PD-L1 expression of ≥50% (31). However, the potential reason for the inferior immunotherapy outcome of patients with cachexia was still unclear. Patients with cachexia were found to have increased antibody clearance, which might be associated with inferior survival of immunotherapy (32). Besides, it should be noted that the molecular mechanisms and pathways that contribute to the onset of cancer cachexia syndrome may also play a role on the immune suppressive characteristics of the tumor microenvironment and impairing the body's ability to mount an effective anti-tumor immunity (26). On the other hand, the deregulation of metabolic homeostasis in patients with cachexia is linked with resistance to ICIs (26).

Our previous study also indicated the effect of longitudinal changes of cachexia on the efficacy of ICIs in esophageal squamous cell cancer (33), and irreversible cachexia showed the poorest efficacy. Thus, the early detection and management of cachexia is important to improve the survival of ES-SCLC patients.

The progressive depletion of host protein stores is at the core of cancer cachexia (34). Due to the depletion of skeletal muscle by the disease, the appearance of cachexia-sarcopenia syndrome frequently precedes the decline in performance status and is linked with alterations in certain biological markers, such as reduced serum albumin level (35). PA, which reflect the changes in protein renewal, conversion and consumption in the body (36), can be

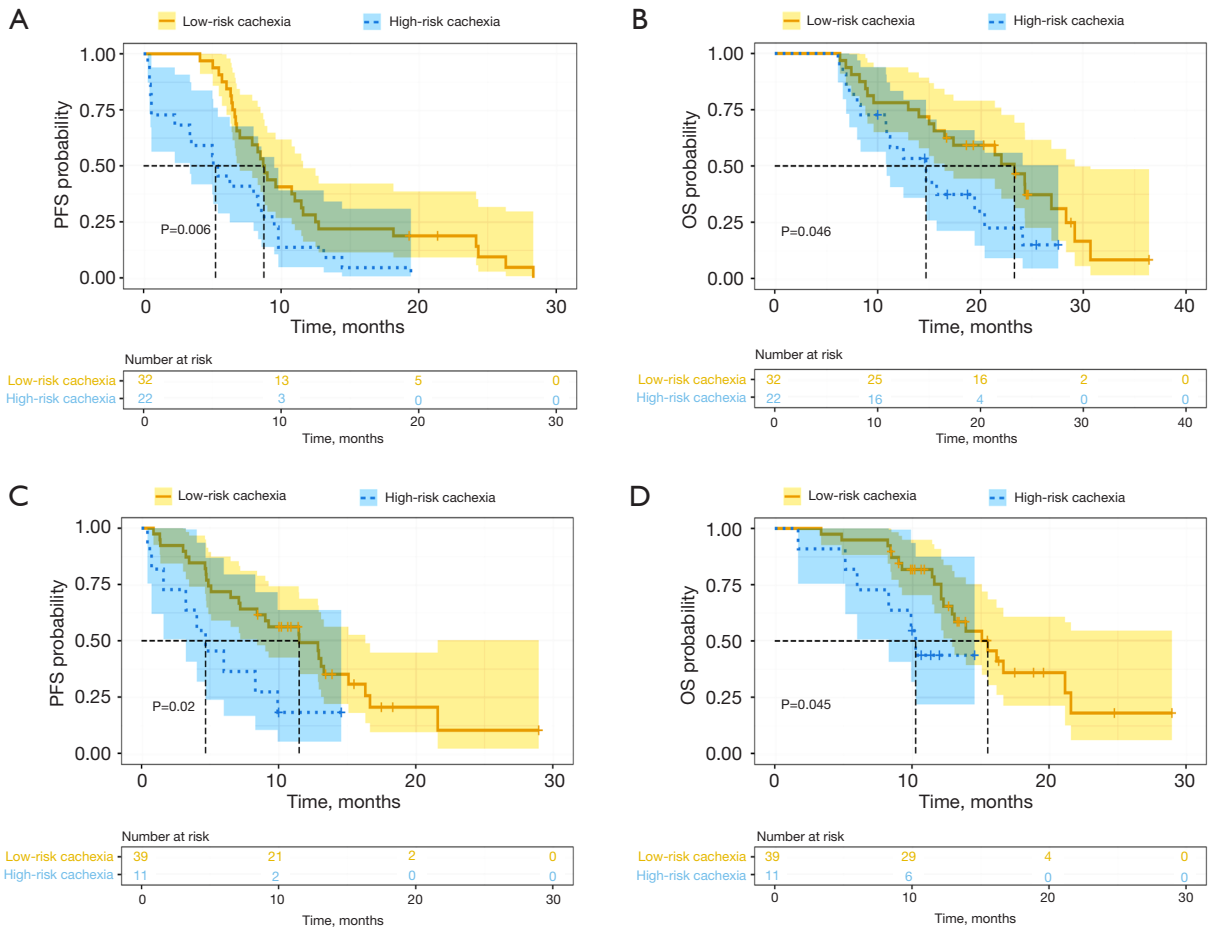

Figure 4 The Kaplan-Meier curves of DL model for PFS and OS. The Kaplan-Meier survival curve of patients with high and low risk cachexia predicted by DL for PFS (A) and OS (B) in the internal validation cohort. The Kaplan-Meier survival curve of patients with high and low risk cachexia predicted by DL for PFS (C) and OS (D) in the external validation cohort. PFS, progression-free survival; OS, overall survival; DL, deep learning.

employed for the evaluation of nutritional and immune status of individuals suffering from cancer. In addition, PA was observed to be linked with the occurrence of cachexia in ES-SCLC patients undergoing immunotherapy in this investigation. Furthermore, the increase of ALC, a measure of systemic inflammatory response, would increase the risk of cachexia (37). The levels of soluble immune mediators including C-reactive protein, pentraxin-3, and osteopontin were found to be associated with the incidence of cachexia (29). However, soluble parameters might be influenced by several factors like diets, lifestyles and others, and more stable stools are needed for the early identification of cachexia.

Sarcopenia, which was provided by a single cross-sectional skeletal muscle area, has been argued to reflect the advanced disease status, deteriorated physical condition and cachexia of cancer patients (35,38). Skeletal muscle and fat mass were quantified using CT image analysis of the L3 vertebrae. Due to its accuracy, the skeletal muscle of the L3 vertebrae has been suggested by The European Association for the Study of the Liver (EASL) Clinical Practice Guidelines to evaluate sarcopenia (39). Additionally, radiomics model using PET/CT imaging has been utilized to predict the risk of cachexia in ICIs-treated NSCLC patients, with findings correlated to clinical outcomes (40). Thus, radiomics features of muscles in the L3 vertebrae were exploited to make early detection of cachexia. The results showed that RS performed well in the internal validation cohort but had much lower accuracy in the external validation cohort, which might be attributed to

RS's overfitting.

DL has been widely used to address clinical issues in medical image processing, including CT, PET-CT, and pathology images. DL-based radiomics analysis, as compared to manual image processing, eliminates manual feature extraction and is linked with superior predictive performance. Thus, the DL model for cachexia prediction was built using pre-trained ResNet-50. Our findings showed that the DL model outperformed the external validation cohort, in terms of early detection of cachexia. The data-driven DL model has been discovered to outperform classic radiomics-based methods in automatically extracting task-specific characteristics from radiological images.

In this study, ES-SCLC patients with cachexia have been found to have inferior outcome from immunotherapy. The DL radiomics model was developed for the early and dynamic detection of cachexia, and was also found to have predictive value for the outcome of immunotherapy. The DL model for cachexia may potentially be considered as the biomarker for immunotherapy, enabling the identification of patients who might achieve a durable survival benefit from immunotherapy. It should be noted that there were also some limitations of this study. Firstly, the sample size is relatively small, particularly for evaluating the DL model, which may limit its generalizability. Validation of the model in large sample from multicenter is needed in further studies. Additionally, while the DL model shows promise, its complexity and "black-box" nature may limit clinical acceptance, and further efforts are needed to improve its interpretability.

Conclusions

In summary, the occurrence of cachexia was found to be correlated with poor survival outcomes in ES-SCLC patients who received immunotherapy. The DL model from the pre-treatment CT images has the potential to function as a predictive biomarker for the identification of patients at risk of developing cachexia, and may prove valuable in the optimization of treatment plans.

Acknowledgments

Funding: This research was supported by National Natural Science Foundation of China (Grant No. 82172865), Start-up fund of Shandong Cancer Hospital (Grant No. 2020-B14), Clinical Research Special Fund of Wu Jieping Medical Foundation (Grant Nos. 320.6750.2021-02-51 and 320.6750.2021-17-13) and the Natural Science Foundation of Shandong Province (Nos. ZR2020LZL019 and ZR2020QH244).

Footnote

Reporting Checklist: The authors have completed the TRIPOD reporting checklist. Available at https://tlcr.amegroups.com/article/view/10.21037/tlcr-24-543/rc

Data Sharing Statement: Available at https://tlcr.amegroups.com/article/view/10.21037/tlcr-24-543/dss

Peer Review File: Available at https://tlcr.amegroups.com/article/view/10.21037/tlcr-24-543/prf

Conflicts of Interest: All authors have completed the ICMJE uniform disclosure form (available at https://tlcr.amegroups.com/article/view/10.21037/tlcr-24-543/coif). The authors have no conflicts of interest to declare.

Ethical Statement: The authors are accountable for all aspects of the work in ensuring that questions related to the accuracy or integrity of any part of the work are appropriately investigated and resolved. This research, a retrospective and multi-institutional investigation, received approval from the Ethics Committee of Shandong Cancer Hospital and Institute (No. 2023010002) and the Institutional Review Board at each participating hospital. All participating institutions were informed and agreed on the study. The research was conducted in accordance with the Declaration of Helsinki (as revised in 2013), and given that it is a retrospective study, individual consent for this retrospective analysis was waived.

References

1. Nicholson AG, Chansky K, Crowley J, et al. The

International Association for the Study of Lung Cancer Lung Cancer Staging Project: Proposals for the Revision of the Clinical and Pathologic Staging of Small Cell Lung Cancer in the Forthcoming Eighth Edition of the TNM Classification for Lung Cancer. J Thorac Oncol 2016;11:300-11.
2. Zugazagoitia J, Paz-Ares L. Extensive-Stage Small-Cell Lung Cancer: First-Line and Second-Line Treatment Options. J Clin Oncol 2022;40:671-80.
3. Tian Y, Ma J, Jing X, et al. Radiation therapy for extensive-stage small-cell lung cancer in the era of immunotherapy. Cancer Lett 2022;541:215719.
4. Rudin CM, Awad MM, Navarro A, et al. Pembrolizumab or Placebo Plus Etoposide and Platinum as First-Line Therapy for Extensive-Stage Small-Cell Lung Cancer: Randomized, Double-Blind, Phase III KEYNOTE-604 Study. J Clin Oncol 2020;38:2369-79.
5. Li H, Zhao Y, Ma T, et al. Radiotherapy for extensive-stage small-cell lung cancer in the immunotherapy era. Front Immunol 2023;14:1132482.
6. Paz-Ares L, Dvorkin M, Chen Y, et al. Durvalumab plus platinum-etoposide versus platinum-etoposide in first-line treatment of extensive-stage small-cell lung cancer (CASPIAN): a randomised, controlled, open-label, phase 3 trial. Lancet 2019;394:1929-39.
7. Goldman JW, Dvorkin M, Chen Y, et al. Durvalumab, with or without tremelimumab, plus platinum-etoposide versus platinum-etoposide alone in first-line treatment of extensive-stage small-cell lung cancer (CASPIAN): updated results from a randomised, controlled, open-label, phase 3 trial. Lancet Oncol 2021;22:51-65.
8. Yang K, Halima A, Chan TA. Antigen presentation in cancer - mechanisms and clinical implications for immunotherapy. Nat Rev Clin Oncol 2023;20:604-23.
9. Argilés JM, López-Soriano FJ, Stemmler B, et al. Cancer-associated cachexia - understanding the tumour macroenvironment and microenvironment to improve management. Nat Rev Clin Oncol 2023;20:250-64.
10. Biswas AK, Acharyya S. Understanding cachexia in the context of metastatic progression. Nat Rev Cancer 2020;20:274-84.
11. Liu X, Li S, Cui Q, et al. Activation of GPR81 by lactate drives tumour-induced cachexia. Nat Metab 2024;6:708-23.
12. Takenaka Y, Oya R, Takemoto N, et al. Predictive impact of sarcopenia in solid cancers treated with immune checkpoint inhibitors: a meta-analysis. J Cachexia Sarcopenia Muscle 2021;12:1122-35.
13. Degens JHRJ, Dingemans AC, Willemsen ACH, et al. The prognostic value of weight and body composition changes in patients with non-small-cell lung cancer treated with nivolumab. J Cachexia Sarcopenia Muscle 2021;12:657-64.
14. Go SI, Park MJ, Lee GW. Clinical significance of the cachexia index in patients with small cell lung cancer. BMC Cancer 2021;21:563.
15. Go SI, Jeon H, Park SW, et al. Low pre-treatment nutritional index is significantly related to poor outcomes in small cell lung cancer. Thorac Cancer 2018;9:1483-91.
16. Kim EY, Kim YS, Park I, et al. Prognostic Significance of CT-Determined Sarcopenia in Patients with Small-Cell Lung Cancer. J Thorac Oncol 2015;10:1795-9.
17. Baazim H, Antonio-Herrera L, Bergthaler A. The interplay of immunology and cachexia in infection and cancer. Nat Rev Immunol 2022;22:309-21.
18. Shachar SS, Williams GR, Muss HB, et al. Prognostic value of sarcopenia in adults with solid tumours: A meta-analysis and systematic review. Eur J Cancer 2016;57:58-67.
19. Yu Q, Ning Y, Wang A, et al. Deep learning-assisted diagnosis of benign and malignant parotid tumors based on contrast-enhanced CT: a multicenter study. Eur Radiol 2023;33:6054-65.
20. van der Voort SR, Incekara F, Wijnenga MMJ, et al. Combined molecular subtyping, grading, and segmentation of glioma using multi-task deep learning. Neuro Oncol 2023;25:279-89.
21. Fu N, Fu W, Chen H, et al. A deep-learning radiomics-based lymph node metastasis predictive model for pancreatic cancer: a diagnostic study. Int J Surg 2023;109:2196-203.
22. Blum D, Stene GB, Solheim TS, et al. Validation of the Consensus-Definition for Cancer Cachexia and evaluation of a classification model--a study based on data from an international multicentre project (EPCRC-CSA). Ann Oncol 2014;25:1635-42.
23. Ryan AM, Power DG, Daly L, et al. Cancer-associated malnutrition, cachexia and sarcopenia: the skeleton in the hospital closet 40 years later. Proc Nutr Soc 2016;75:199-211.
24. Yushkevich PA, Piven J, Hazlett HC, et al. User-guided 3D active contour segmentation of anatomical structures: significantly improved efficiency and reliability. Neuroimage 2006;31:1116-28.
25. Jo H, Yoshida T, Horinouchi H, et al. Prognostic significance of cachexia in advanced non-small cell lung cancer patients treated with pembrolizumab. Cancer Immunol Immunother 2022;71:387-98.

26. Rounis K, Makrakis D, Gioulbasanis I, et al. Cancer Cachexia and Antitumor Immunity: Common Mediators and Potential Targets for New Therapies. Life (Basel) 2022;12:880.
27. Coss CC, Clinton SK, Phelps MA. Cachectic Cancer Patients: Immune to Checkpoint Inhibitor Therapy? Clin Cancer Res 2018;24:5787-9.
28. Turcott JG, Martinez-Samano JE, Cardona AF, et al. The Role of a Cachexia Grading System in Patients with Non-Small Cell Lung Cancer Treated with Immunotherapy: Implications for Survival. Nutr Cancer 2021;73:794-801.
29. Murata D, Azuma K, Matsuo N, et al. Survival and biomarkers for cachexia in non-small cell lung cancer receiving immune checkpoint inhibitors. Cancer Med 2023;12:19471-9.
30. Madeddu C, Busquets S, Donisi C, et al. Effect of Cancer-Related Cachexia and Associated Changes in Nutritional Status, Inflammatory Status, and Muscle Mass on Immunotherapy Efficacy and Survival in Patients with Advanced Non-Small Cell Lung Cancer. Cancers (Basel) 2023;15:1076.
31. Morimoto K, Uchino J, Yokoi T, et al. Impact of cancer cachexia on the therapeutic outcome of combined chemoimmunotherapy in patients with non-small cell lung cancer: a retrospective study. Oncoimmunology 2021;10:1950411.
32. Vu TT, Kim K, Manna M, et al. Decoupling FcRn and tumor contributions to elevated immune checkpoint inhibitor clearance in cancer cachexia. Pharmacol Res 2024;199:107048.
33. Li H, Li B, Wang X, et al. Effect of longitudinal changes of cachexia on the efficacy and toxicity of immune checkpoint inhibitors in esophageal squamous cell cancer (ESCC) patients. Nutrition 2024;124:112462.
34. Arends J. Malnutrition in cancer patients: Causes, consequences and treatment options. Eur J Surg Oncol 2024;50:107074.
35. Fearon K, Strasser F, Anker SD, et al. Definition and classification of cancer cachexia: an international consensus. Lancet Oncol 2011;12:489-95.
36. Davis CJ, Sowa D, Keim KS, et al. The use of prealbumin and C-reactive protein for monitoring nutrition support in adult patients receiving enteral nutrition in an urban medical center. JPEN J Parenter Enteral Nutr 2012;36:197-204.
37. Stephens NA, Skipworth RJ, Fearon KC. Cachexia, survival and the acute phase response. Curr Opin Support Palliat Care 2008;2:267-74.
38. Islam S, Kanavati F, Arain Z, et al. Fully automated deep-learning section-based muscle segmentation from CT images for sarcopenia assessment. Clin Radiol 2022;77:e363-71.
39. European Association for the Study of the Liver. Electronic address: easloffice@easloffice; . EASL Clinical Practice Guidelines on nutrition in chronic liver disease. J Hepatol 2019;70:172-93.
40. Mu W, Katsoulakis E, Whelan CJ, et al. Radiomics predicts risk of cachexia in advanced NSCLC patients treated with immune checkpoint inhibitors. Br J Cancer 2021;125:229-39.

Cite this article as: Song R, Li B, Wang X, Fan X, Zheng Z, Zheng Y, He J, Wang C, Wang L. Construction and validation of deep learning model for cachexia in extensive-stage small cell lung cancer patients treated with immune checkpoint inhibitors: a multicenter study. Transl Lung Cancer Res 2024;13(11):2958-2971. doi: 10.21037/tlcr-24-543